IMPLEMENTATION AND BENCHMARKING OF SEISMIC PROTECTIVE DEVICES IN MASTODON

Sai Sharath Parsi[1], Manish Kumar[2], Manish Kumar[3], Chandrakanth Bolisetti[4], Justin Coleman[5] and Andrew S Whittaker[6]

[1]PhD Student, Department of Civil, Structural and Environmental Engineering, University at Buffalo, State University of New York, Buffalo, NY, USA, saishara@buffalo.edu
[2]Assistant Professor, Department of Civil Engineering, Indian Institute of Technology, Bombay, India
[3]Assistant Professor, Department of Civil Engineering, Indian Institute of Technology, Gandhinagar, India
[4]Scientist, Facility Risk Group, Idaho National Laboratory, Idaho Falls, ID, USA
[5]Senior Technical Advisor for Microreactors, Idaho National Laboratory, Idaho Falls, ID, USA
[6]SUNY Distinguished Professor and MCEER Director, Department of Civil, Structural and Environmental Engineering, University at Buffalo, State University of New York, Buffalo, NY, USA

ABSTRACT

Seismic (base) isolation and damping systems can mitigate the effects of extreme earthquake shaking on buildings, and bridges, and mission-critical infrastructure such as nuclear power plants. Recent studies have indicated that nonlinear seismic isolation systems can reduce seismic risk and the overnight capital cost of nuclear structures but their use has been impeded by the lack of verified and validated numerical models. This paper describes the implementation of numerical models of lead-rubber and Friction Pendulum bearings, and nonlinear fluid viscous dampers in MASTODON. Examples that demonstrate the use of these elements in MASTODON are presented for both static and dynamic (earthquake) load cases. A code-to-code comparison is used for implementing and benchmarking these elements in MASTODON, using results from identical simulations in ABAQUS and OpenSees.

INTRODUCTION

The recently published report *The Future of Nuclear Energy in a Carbon Constrained World* (Buongiorno *et al.*, 2018) identifies the importance of nuclear power in future global green energy production. Unfortunately, an expanded role for nuclear energy is currently hampered by the high overnight capital cost of constructing nuclear power plants (NPPs). One of the key cost drivers for new build NPPs is the seismic load case, with anecdotal evidence suggesting an increase in overnight capital cost of 30+%. Yu *et al.* (2018) showed that deployment of seismic protective devices such as base isolators reduced both seismic demand and seismic risk, leading to significant cost savings. Elastomeric (lead-rubber and low damping rubber) and Friction Pendulum bearings, and fluid viscous dampers, are seismic protective devices that are widely used in commercial buildings in the United States. Although these devices have been applied to certain classes of critical infrastructure in past few decades, they have not been implemented in nuclear facilities in the United States, in part because they lack verified and validated numerical models. Verified and validated models are a pre-requisite for seismic analysis of NPPs in the United States. One challenge associated with modelling these protective devices is that their properties may evolve during earthquake shaking as a result of dissipation of energy. High-fidelity mathematical models that account for these changes will be required for analysis, design, and risk assessment of seismically isolated NPPs (Kammerer *et al.*, 2019).

Kumar *et al.* (2015a; 2018; 2019a) developed an advanced mathematical model of a lead-rubber bearing and implemented it in ABAQUS (Dassault Systèmes, 2018) through the user element (UEL) subroutine *LeadRubberX*; in OpenSees (Mazzoni *et al.*, 2018) with the element *LeadRubberX*; and in LS-DYNA (LSTC, 2013) with the material **MAT_SEISMIC_ISOLATOR (ITYPE 3)*. Kumar *et al.* (2015b; 2019b) developed a numerical model for Friction Pendulum bearings and implemented it in OpenSees with the element *FPBearingPTV*. These four numerical models were verified and validated following ASME best practice (ASME, 2006).

Reinhorn *et al.* (1995) developed constitutive relationships for nonlinear fluid viscous dampers (FVDs) with stiffness dependency, which Akcelyan *et al.* (2018) implemented in OpenSees.

This paper describes the implementation of lead-rubber and Friction Pendulum isolators, and nonlinear fluid viscous damper elements in the open-source application MASTODON: Multi-hazard Analysis for STOchastic time-DOmaiN phenomena (Coleman *et al.*, 2017). MASTODON is being developed, with an NQA-1 (ASME, 2017) pedigree, at the Idaho National Laboratory to perform seismic analysis and risk calculations for safety-related nuclear facilities. MASTODON is hosted on GitHub (https://github.com/idaholab/mastodon) and this site includes source codes, test problems and documentation. MASTODON is currently capable of fault-rupture simulations, source-to-site wave propagation, nonlinear seismic site-response analysis and 3-D soil-structure-interaction (SSI) (Baltaji *et al.*, 2017), and seismic probabilistic risk assessment. Seismic isolator and nonlinear viscous damper elements are added here. A code-to-code comparison is used for implementing and benchmarking the isolator elements in MASTODON, using results from identical simulations of verified and validated numerical models in ABAQUS and OpenSees.

LEAD-RUBBER ISOLATOR

The lead-rubber (LR) isolator consists of vertically stacked, alternating layers of rubber and steel shims, end plates at the top and bottom, and a central, cylindrical lead core. Three-dimensional continuum models for these elements are computationally expensive and impractical for use in nonlinear response-history analysis and so the discrete, two-node model developed by Kumar *et al.* (2014) for LR isolators is implemented in MASTODON. This model has six degrees-of-freedom at each node and the bearing stiffness in axial, shear and rotational directions are represented using nonlinear springs.

Mathematical model

Key aspects of the Kumar *et al.* (2015a) numerical model are described here. The behaviour of LR bearings in compression is well-established. The composite action of the rubber and the steel shims results in high axial stiffness. The LR bearing buckles under high axial loads. Koh and Kelly (1987) developed an expression to calculate the critical buckling load in the undeformed configuration. Later, Warn and Whittaker (2006) experimentally confirmed that the buckling load varies as a function of shear deformation and they proposed simplified expressions that are implemented in MASTODON. In tension, the rubber cavitates: an expansion of existing voids or defects in the material. The bearing exhibits linear behaviour until the point of cavitation. Kumar *et al.* (2014) developed a phenomenological model to simulate the post-cavitation behaviour of LR bearings in tension and it is also implemented here.

The behaviour of LR isolator in shear is a combination of the hysteretic behaviour of the lead core and viscoelastic behaviour of the rubber. The model proposed by Park *et al.* (1986) and extended by Nagarajaiah *et al.* (1989) is used to model the hysteretic behaviour of the lead core. The behaviour of the rubber is characterized by its elastic stiffness and equivalent viscous damping. The model captures the effects of heating of the lead core under reversed cyclic loading using the equations proposed by Kalpakidis and Constantinou (2009). The coupled horizontal and vertical response of the LR isolator affects behavior

at high axial loads and large shear displacements. The shear stiffness of a LR bearing reduces if the axial load is close to the critical buckling load (Kelly, 1993). Warn *et al.* (2007) observed a reduction in the vertical stiffness of the bearing with increasing shear displacement. The numerical model accounts for all of these coupled behaviors. The model assumes linear response in the torsional and other rotational (rocking) directions.

Implementation, results and benchmarking

The lead-rubber (LR) isolator material should be used with a two-node beam or link type elements in MASTODON. For each subdomain (part of the mesh), which may contain several link elements, the properties are defined by creating 'Material' and 'Kernel' blocks in the input file. The `StressDivergenceIsolator` Kernel computes the Jacobian and residual forces in the isolator element. The `ComputeIsolatorDeformation` Material block inputs the global orientation of the element and computes the deformations in the isolator element. The `ComputeLRIsolatorElasticity` Material block inputs the geometrical and material properties of the bearing and computes the force vector and stiffness matrix for the isolator element. This material, by default, simulates cavitation in tension, heating in the lead core, variation in buckling load with shear displacement, and coupling between horizontal and vertical responses of the bearing. Users are also provided with options to switch off these behaviours in the analysis. The use of the lead-rubber isolator element in MASTODON is demonstrated here using three examples. Results of these example simulations are benchmarked with the verified and validated numerical model in ABAQUS.

For these example calculations, a two-node isolator element is analysed, with its bottom node fixed and the rotational degrees-of-freedom at the top node restrained. The properties of the LR bearing used in Examples 1, 2 and 3 are presented in Table 1 of the Appendix. The switches for cavitation, heating, buckling load variation and coupled response in the ComputeLRIsolatorElasticity material are set to true.

In Example 1, a cyclic triangular pulse with increasing displacement amplitudes of 5 mm, 35 mm, and 105 mm is applied in the vertical (local-X) direction at the top node using the `PresetDisplacement` boundary condition in MASTODON. Simultaneously, the top node is also linearly displaced in shear (local-y direction) to an amplitude of 305 mm to characterize the coupled response. Identical to ABAQUS, the numerical model in MASTODON is able to simulate cavitation and post-cavitation behaviour. The buckling load in cycle 2 is less than that in cycle 1 due to the increasing shear displacement of the bearing: see Figure 1a. In Example 2, a sinusoidal displacement history with an amplitude of 150 mm and a frequency of 0.5 Hz is applied in shear (local-Y) at the top node. To simulate gravity loadings, a constant axial force 1439 kN is applied at the top node using 'NodalKernel' of the type `UserForcingFunctionNodalKernel`. The hysteretic behaviour of the LR bearing in the horizontal (shear) directions is presented in Figure 1b. In Figure 1b, the characteristic strength of the bearing reduces with increasing cycling due to the heating of the lead core. The MASTODON and ABAQUS results are in excellent agreement for Examples 1 and 2.

In Example 3, the isolator element is subjected to earthquake shaking. The horizontal and vertical components of a sample ground motion[1] are applied to the bottom node using the `PresetAcceleration` boundary condition. To simulate gravity loadings, a mass of 146890 kg is assigned to the top node using a NodalKernel of the type `NodalTranslationInertia`. Gravity load is applied to the model before the seismic load case is imposed. The Newmark-Beta integration scheme ($\beta = 0.25$, $\gamma = 0.5$) is employed and no additional damping is assigned. When heating effects are activated, a smaller time step, in range of 0.0001 sec is recommended to achieve numerical convergence. Figure 2

---

[1] See: https://github.com/idaholab/mastodon/tree/devel/test/tests/materials/lr_isolator

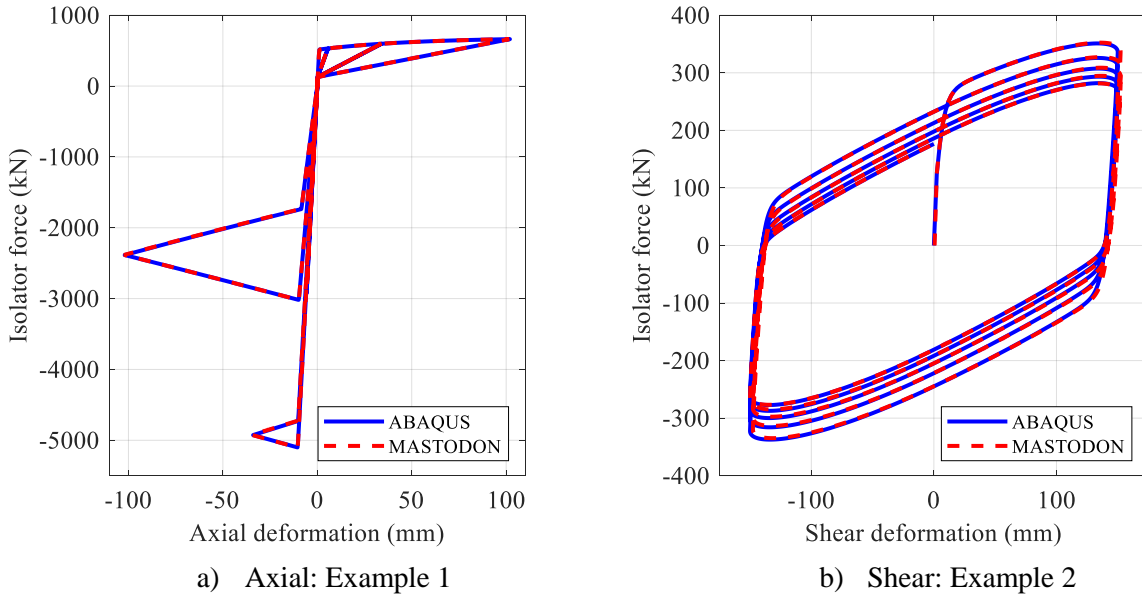shows the seismic response of the LR bearing in shear. Again, the MASTODON and ABAQUS responses are identical.

a)   Axial: Example 1
b)   Shear: Example 2

Figure 1. Response of a LR bearing in MASTODON and ABAQUS: Examples 1 and 2
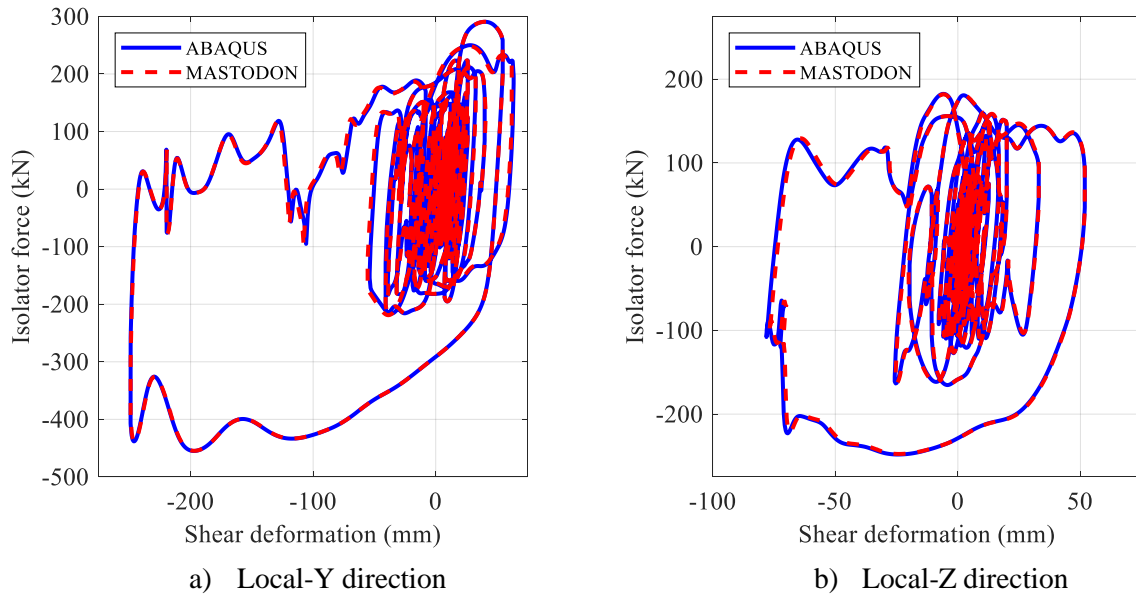

a)   Local-Y direction
b)   Local-Z direction

Figure 2. Response of a LR bearing subjected to the prescribed seismic loading: Example 3

FRICTION PENDULUM ISOLATOR

A single concave Friction Pendulum (FP) isolator consists of a spherical sliding surface, a slider coated with PTFE-type composite material, and a housing plate. Kumar *et al.* (2015b) developed a mathematical framework to simulate the behaviour of FP bearings and it is now implemented in MASTODON. Similar to the numerical model of the lead-rubber bearing, the FP bearing element is also a discrete two-node model

with six degrees-of-freedom at each node and the bearing stiffness in axial, shear and rotational directions are represented using nonlinear springs (Kumar *et al.*, 2014).

Mathematical model

A bilinear force-displacement relation in shear is assumed for the FP bearing. The characteristic strength of the bearing is defined as the product of coefficient of sliding friction of the composite (μ), the instantaneous axial pressure on the bearing (p), and the plan area of the slider. The post-elastic stiffness is governed by the effective radius of curvature of the sliding surface (R) and the axial load. During an earthquake, the coefficient of sliding friction changes continuously and it depends on the sliding velocity (v), axial pressure (p), and the instantaneous temperature at the sliding interface (T). The sliding velocity and axial pressure are governed by the input excitation and the response of the superstructure. The temperature at the sliding surface further depends on various parameters, as shown in equation (1):

$$T(t) = f(\mu, v, p, D, k) \tag{1}$$

where k is the thermal conductivity and D is the thermal diffusivity of the composite. Kumar *et al.* (2015b) developed a framework to account for the variation in the coefficient of sliding friction due to the combined effects of velocity, pressure, and temperature, and it is adopted here. The FP bearing exhibits large axial, rotational and torsional stiffness, and so these are modelled using linear elastic springs.

Implementation, results and benchmarking

The FP isolator material in MASTODON should be used with a two-node beam or link type elements. The material is defined in the input file using the `ComputeIsolatorDeformation` and `ComputeFPIsolatorElasticity` 'Material' blocks, and the `StressDivergenceIsolator` 'Kernel' blocks. The `ComputeFPIsolatorElasticity` block inputs the FP bearing properties and computes the force vector and the stiffness matrix. The material is provided with user input switches to explicitly model the dependency of coefficient of friction on sliding velocity, axial pressure and temperature

The use of the FP bearing element in MASTODON is demonstrated using the following examples. In Example 4, a two-node link element is used for calculations. The bottom node is fixed and rotations at the top node are restrained. The axial and rotational stiffness (input to the ComputeFPIsolatorElasticity material) are assigned the default value of 10^{14} N/m (in SI units) in MASTODON. When a different unit system is used, the user is advised to enter a high stiffness (i.e., 2 to 3 times the shear stiffness) to simulate rigid behaviour in these directions. A gravity load of 6285 kN is applied at the top node to simulate the axial load on the bearing. The bearing properties used for this example are presented in Table 2 of the Appendix. Here, the coefficient of friction is modelled as a function of temperature only for the code-to-code comparison. A quasi-static sinusoidal load with a frequency of 0.5 Hz and increasing displacement amplitudes of 100 mm, 150 mm, and 200 mm is applied at the top node using the `PresetDisplacement` boundary condition. The MASTODON results are compared with those from OpenSees. As observed in Figure 3, the characteristic strength of the bearing reduces with repeated cycling due to the effect of temperature on the coefficient of sliding friction.

In Example 5, the FP bearing is subjected to earthquake shaking in both the horizontal and vertical directions. A mass of 64045 kg is assigned to the top node to simulate the mass of superstructure. The `PresetAcceleration` boundary condition is used to apply the ground motions[2] at the bottom node. The Newmark-Beta algorithm (β = 0.25 and γ = 0.5) is employed for time integration. No additional

---

[2] See: https://github.com/idaholab/mastodon/tree/devel/test/tests/materials/fp_isolator

damping is imposed. The responses of the FP bearing in shear under seismic excitation are shown in Figure 4. The responses calculated using the models in OpenSees and MASTODON are identical for Examples 4 and 5.
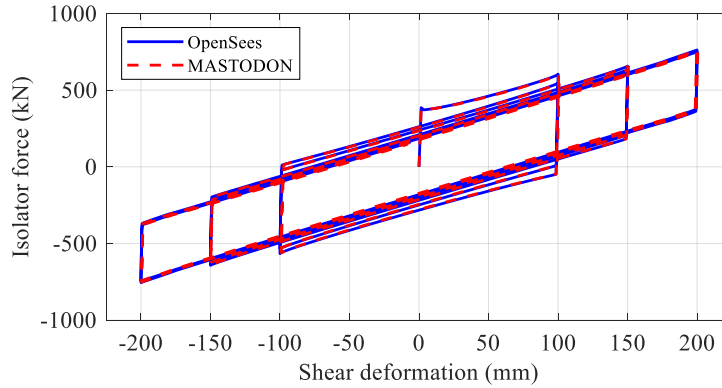

Figure 3. Response of the FP bearing to the prescribed cyclic loading in shear: Example 4
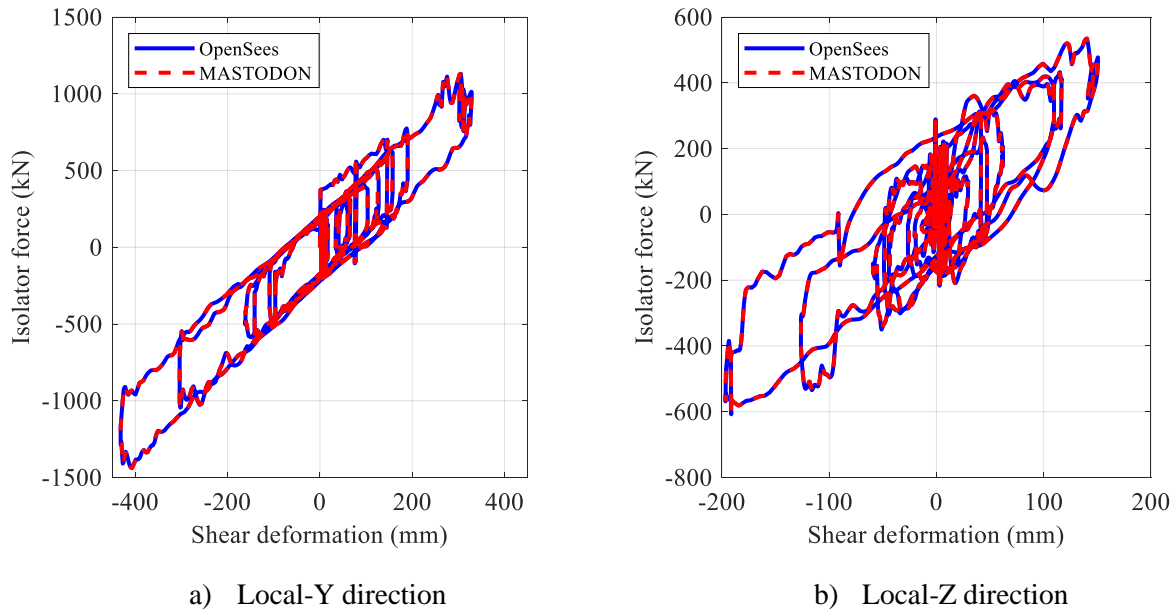

a) Local-Y direction

b) Local-Z direction

Figure 4. Seismic response of the FP bearing in shear: Example 5

NONLINEAR FLUID VISCOUS DAMPER

Nonlinear fluid viscous dampers (FVDs) are used in framed buildings to mitigate earthquake-induced vibrations and damage. Those fluid viscous dampers used for seismic applications in the United States display internal axial resistance that is proportional to a fractional power of relative velocity across the damper. These dampers exhibit some stiffness (see Figure 5) and complex mathematical models are required to simulate their nonlinear behaviour (Reinhorn *et al.*, 1995). A two-node truss model with one degree of freedom (along its axis) at each node is used to implement a FVD element in MASTODON.

Mathematical model

A FVD operates on the principle of fluid flow through orifices, creating a differential pressure across the piston head. This differential pressure develops an internal resisting force that is proportional to the velocity across the damper, as shown in equation (2) (Reinhorn *et al.*, 1995). The damping coefficient (C_d) and the velocity exponent (α) characterize the damper behaviour. For $\alpha = 1$, equation (2) models a linear damper. For seismic applications in the United States, the typical range for α is between 0.3 and 1.0. Reinhorn *et al.* (1995) developed an expression for the force in a FVD with axial stiffness and it is implemented in MASTODON. The FVD behavior is idealized as a linear spring and nonlinear dashpot connected in series, and is represented using a Maxwell formulation. The constitutive relationship between force and velocity using Maxwell model is shown in the equation (3).

$$F_d(t) = C_d |\dot{u}(t)|^{\alpha} sign(\dot{u}(t)) \tag{2}$$

$$F_d'(t) = \left(\dot{u}(t) - \text{sgn}(F_d(t)) \left(\frac{|F_d(t)|}{C_d} \right)^{\frac{1}{\alpha}} \right) K_s \qquad F_d(t_o) = F_o \tag{3}$$

a) Overall damper behaviour   b) Stiffness component   c) Damping component
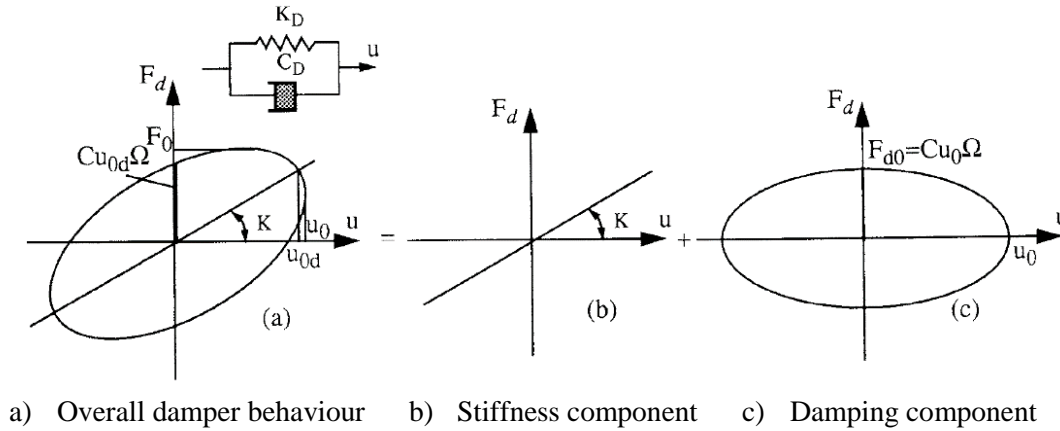
Figure 5. Linear damping and stiffness device (Reinhorn *et al.*, 1995)

Dormand and Prince (1980) proposed an efficient iterative integration scheme (known as Dormand Prince (DP54)), to solve a generalized initial-value problem of the form shown in equation (3). Akcelyan *et al.* (2018) developed a framework to obtain the numerical solution of equation (3) using the DP54 algorithm and it is implemented in MASTODON.

Implementation, results and benchmarking

The `ComputeFVDamperElasticity` 'Material' block should be used with a two-node link type elements in MASTODON to simulate the behaviour of a nonlinear FVD. The orientation of the element, damping coefficient, stiffness and velocity exponent are provided as inputs in this material block. The `StressDivergenceDamper` 'Kernel' calculates the Jacobian and the residual forces in the damper element. The following examples demonstrate the use of a nonlinear FVD element in MASTODON.

Example 6 uses a two-node damper element with its bottom node restrained. A sinusoidal displacement history with a frequency of 0.5 Hz and increasing amplitudes of 12 mm, 24 mm and 36 mm is applied at the top node along the damper axis. Two test cases, with varying C_d and α, and constant

stiffness of 300 x 10^6 N/m are considered. Figure 6 compares the MASTODON results with those from simulations using the OpenSees model. The agreement is excellent.
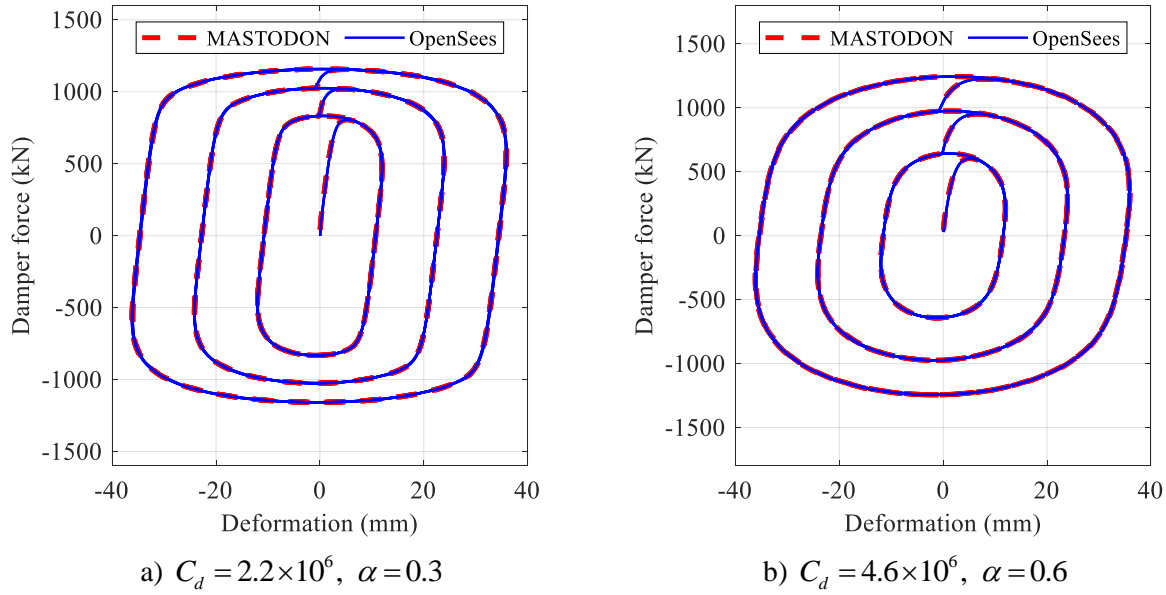

a) $C_d = 2.2 \times 10^6$, $\alpha = 0.3$

b) $C_d = 4.6 \times 10^6$, $\alpha = 0.6$

Figure 6. Response of a nonlinear FVD element to a sinusoidal displacement history: Example 6

a) Single-bay, single-story frame
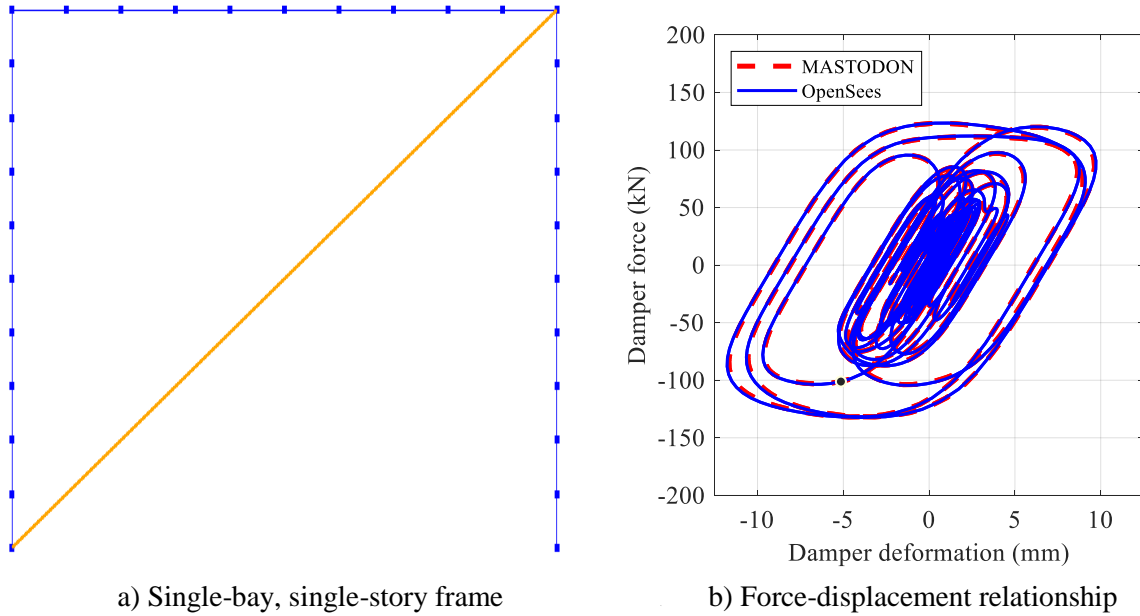
b) Force-displacement relationship

Figure 7. Response of a nonlinear FVD element to the prescribed seismic loading: Example 7

Example 7 utilizes a single-bay, single-story frame, 5 m long and 3 m high, with a diagonally oriented FVD element, as shown in Figure 7a. The reinforced concrete beam and columns (300 mm wide and 300 mm deep each) are linear-elastic and modelled using Euler-Bernoulli formulation. The properties for the beam and columns are defined using `LineElementMaster` block. The properties of the damper used in this example are presented in Table 3 of the Appendix. A reactive mass of 50 tons is lumped at the floor nodes using NodalKernel of the type `NodalTranslationInertia`. Figure 7b shows the force-

deformation plot in the damper element when the frame is subjected to a horizontal earthquake shaking[3]. The MASTODON results are in excellent agreement with those from the OpenSees simulations.

CONCLUSIONS

Numerical models for lead-rubber and Friction Pendulum isolators, and nonlinear fluid viscous dampers are implemented in MASTODON and benchmarked using results of identical models in ABAQUS and OpenSees. The material for the LR bearing captures cavitation, degradation in characteristic strength due to heating, and coupling of horizontal and vertical responses. The FP bearing material accommodates the influence of sliding velocity, axial pressure and temperature (heating) on the characteristic strength and stiffness of the bearing. The nonlinear FVD material can include axial stiffness. The newly added capabilities to MASTODON will allow the analysis of NPPs and systems and components protected by isolators and fluid viscous dampers.

ACKNOWLEDGMENTS

REFERENCES

Akcelyan, S., Lignos, D. G., and Hikino, T. (2018). "Adaptive numerical method algorithms for nonlinear viscous and bilinear oil damper models subjected to dynamic loading." *Soil Dynamics and Earthquake Engineering*, 113, 488-502.

American Society of Mechanical Engineers (ASME). (2006). "Guide for verification and validation in computational solid mechanics." *ASME V&V 10–2006*, New York, NY.

American Society of Mechanical Engineers (ASME). (2017). "Quality assurance requirements for nuclear facility applications." *NQA-1-2017*, New York, NY.

Baltaji, O., Numanoglu, O., Veeraraghavan, S., Hashash, Y., Coleman, J. L., and Bolisetti, C. (2017). "Non-linear time domain site response and soil structure analyses for nuclear facilities using MASTODON." *Transactions*, 24th International Conference on Structural Mechanics in Reactor Technology (SMiRT 24), Busan, S. Korea, August 2017.

Buongiorno, J., Corradini, M., Parsons, J., and Petti, D. (2018). "The future of nuclear energy in a carbon constrained world - an interdisciplinary MIT study." MIT Energy Initiative, Massachusetts Institute of Technology, Cambridge, MA, USA. http://energy.mit.edu/research/future-nuclear-energy-carbon-constrained-world

Coleman, J. L., Slaughter, A., Veeraraghavan, S., Bolisetti, C., Numanoglu, O. A., Spears, R., Hoffman, W., and Kurt, E. G. (2017). "MASTODON Theory Manual." INL/EXT-17-41930, Idaho National Laboratory, Idaho Falls, ID. https://mooseframework.org/mastodon

Dassault Systèmes (Dassault Systèmes). (2018). Computer Program ABAQUS - Finite Element Analysis Software - Version 2018. Providence, RI.

Dormand, J. R., and Prince, P. J. (1980). "A family of embedded Runge-Kutta formulae." *Journal of Computational and Applied Mathematics*, 6(1), 19-26.

Kalpakidis, I. V., and Constantinou, M. C. (2009). "Effects of heating on the behavior of lead-rubber bearings. I: Theory." *Journal of Structural Engineering*, 135(12), 1440-1449.

---

[3] See: https://github.com/idaholab/mastodon/tree/devel/test/tests/materials/fv_damper

Kammerer, A. M., Whittaker, A. S., and Constantinou, M. C. (2019). "Technical considerations for seismic isolation of nuclear facilities." NUREG/CR-7253, United States Nuclear Regulatory Commission, Washington, DC.

Kelly, J. M. (1993). "Earthquake-resistant design with rubber." Springer-Verlag, London.

Koh, C. G., and Kelly, J. M. (1987). "Effects of axial load on elastomeric bearings." Technical Report EERC/UBC-86/12, Earthquake Engineering Research Center, University of California, Berkeley, CA.

Kumar, M., Whittaker, A. S., and Constantinou, M. C. (2014). "An advanced numerical model of elastomeric seismic isolation bearings." *Earthquake Engineering & Structural Dynamics*, 43(13), 1955-1974.

Kumar, M., Whittaker, A. S., and Constantinou, M. C. (2015a). "Seismic isolation of nuclear power plants using elastomeric bearings." Technical Report MCEER-15-0008, University at Buffalo, The State University of New York, Buffalo, NY.

Kumar, M., Whittaker, A. S., and Constantinou, M. C. (2015b). "Seismic isolation of nuclear power plants using sliding bearings." Technical Report MCEER-15-0006, University at Buffalo, The State University of New York, Buffalo, NY.

Kumar, M., and Whittaker, A. S. (2018). "Cross-platform implementation, verification and validation of advanced mathematical models of elastomeric seismic isolation bearings." *Engineering Structures*, 175, 926-943.

Kumar, M., Whittaker, A. S., and Constantinou, M. C. (2019a). "Seismic isolation of nuclear power plants using elastomeric bearings." NUREG/CR-7255, United States Nuclear Regulatory Commision, Washington, DC.

Kumar, M., Whittaker, A. S., and Constantinou, M. C. (2019b). "Seismic isolation of nuclear power plants using sliding bearings." NUREG/CR-7254, United States Nuclear Regulatory Commision, Washington, DC.

Livermore Software Technology Corporation (LSTC). (2013). Computer Program LS-DYNA Keyword User's Manual - Version R 7.0. Livermore, CA.

Pacific Earthquake Engineering Research Center (PEER), University of California (Mazzoni, S., McKenna, F., Scott, M. H., and Fenves, G. L.). (2018). Computer Program OpenSees: Open System for Earthquake Engineering Simulation - Version 3.0.3. Berkeley, CA.

Nagarajaiah, S., Reinhorn, A., and Constatinou, M. (1989). "Nonlinear dynamic analysis of three-dimensional base isolated structures (3D-BASIS)." Technical Report NCEER-89-0019, University at Buffalo, The State University of New York, Buffalo, NY.

Park, Y., Wen, Y., and Ang, A. H. S. (1986). "Random vibration of hysteretic systems under bi-directional ground motions." *Earthquake Engineering & Structural Dynamics*, 14(4), 543-557.

Reinhorn, A. M., Li, C., and Constantinou, M. C. (1995). "Experimental & analytical investigation of seismic retrofit of structures with supplemental damping, Part 1: Fluid viscous damping devices." Technical Report NCEER-95-0001, University at Buffalo, The State University of New York, Buffalo, NY.

Warn, G. P., and Whittaker, A. S. (2006). "A study of the coupled horizontal-vertical behavior of elastomeric and lead-rubber seismic isolation bearings." Technical Report MCEER 06-0011, University at Buffalo, The State University of New York, Buffalo, NY.

Warn, G. P., Whittaker, A. S., and Constantinou, M. C. (2007). "Vertical stiffness of elastomeric and lead–rubber seismic isolation bearings." *Journal of Structural Engineering*, 133(9), 1227-1236.

Yu, C.-C., Bolisetti, C., Coleman, J. L., Kosbab, B., and Whittaker, A. S. (2018). "Using seismic isolation to reduce risk and capital costs of safety-related nuclear facilities." *Nuclear Engineering and Design*, 326, 268-284.

APPENDIX

Table 1. Model parameters for the lead-rubber bearing used in Examples 1, 2 and 3

Parameter	Description	Value	Units
fy	yield strength of lead core at room temperature	207160	N
alpha	yield displacement of the bearing	0.038	-
G_rubber	shear modulus of rubber	870000	N/m^2
K_rubber	bulk modulus of rubber	2000000000	N/m^2
D1	inner diameter of bearing	0.1397	m
D2	outer diameter of bearing	0.508	m
ts	thickness of steel shims	0.00476	m
tr	thickness of rubber layer	0.009525	m
n	number of rubber layers	16	-
tc	thickness of rubber cover of the bearing	0.0127	m
kc	cavitation parameter	20	1/m
phi_m	damage index	0.75	-
ac	strength degradation parameter	1	-
cd	viscous damping parameter	0	N-s/m
k_steel	thermal conductivity of steel	50	W/(m-ºC)
a_steel	thermal diffusivity of steel	1.41e-5	m^2/s
rho_lead	density of lead core	11200	kg/m^3
c_lead	specific heat of lead core	130	J/(kg-ºC)

Table 2. Model parameters for the Friction Pendulum bearing used in Examples 4 and 5

Parameter	Description	Value	Units
mu_ref	reference coefficient of friction	0.06	-
p_ref	reference pressure on the bearing	50000000	N/m^2
r_eff	effective radius of curvature	2.235	m
r_contact	radius of slider	0.2	m
uy	yield displacement of bearing	0.001	m
a	rate parameter	100	s/m
diffusivity	thermal diffusivity of steel	4.4e-6	m^2/s
conductivity	thermal conductivity of steel	18	W/(m-ºC)

Table 3. Model parameters for the nonlinear fluid viscous damper used in Examples 6 and 7

Parameter	Description	Value	Units
Cd	damping coefficient	232764	N-s/m
Alpha	velocity exponent	0.35	-
K	stiffness	25000000	N/m